



Published in final edited form as:

Free Radic Biol Med. 2008 March 1; 44(5): 807–814. doi:10.1016/j.freeradbiomed.2007.11.005.

SUSTAINED HYPOXIA MODULATES MITOCHONDRIAL DNA CONTENT IN THE NEONATAL RAT BRAIN

Heung M Lee^{1,2}, George H Greeley Jr.¹, and Ella W Englander^{1,2}

¹ Department of Surgery, University of Texas Medical Branch, Galveston, Texas

² Shriners Hospitals for Children, Galveston, Texas

Abstract

Effects of placental insufficiency and preterm birth on neurodevelopment can be modeled in experimental settings of neonatal hypoxia in rodents. Here, rat pups were reared in reduced oxygen (9.5%) for eleven days, starting on postnatal day three (P3). This led to a significant reduction in brain and body weight gain in hypoxic pups when compared to age matched normoxia reared controls, plausibly reflecting inability to fulfill energetic needs of normal growth and development. Adaptive processes designed to augment energetic capacity in eukaryotes include stimulation of mitochondrial biogenesis. We show that after eleven days of sustained hypoxia, the levels of nuclear respiratory factor 1 (NRF-1) and mitochondrial transcription factor A (Tfam) are elevated and the content of mitochondrial DNA (mtDNA) is greater in the hypoxic P14 pup brain when compared to normoxic conditions. Corresponding immunohistochemical analyses reveal increased density of mtDNA in large cortical neurons. In contrast, no changes in mtDNA content are observed in the brain of pups reared for 24 h (P3–P4) under hypoxic conditions. Together, these data suggest that prolonged inadequate oxygenation may trigger a compensatory increase in neuronal mitochondrial DNA content to partially mitigate compromised energy homeostasis and reduced energetic capacity in the developing hypoxic brain.

Keywords

caloric restriction; mild hypoxia; mitochondrial DNA; neonate; neurodevelopment; nitrotyrosine; nuclear respiratory factor-1

INTRODUCTION

To model neurodevelopmental deficits associated with perinatal hypoxia in humans [1–3], rodent models of hypoxia/ischemia have been established [4–8]. Generally, rodent protocols of perinatal sublethal hypoxia produce adverse effects including reduced rate of brain weight gain and neuronal density as well as enlargement of forebrain ventricles [7–9] reminiscent of outcomes of placental insufficiency and preterm births in humans, where energetic capacity is compromised.

Corresponding author: Ella W Englander, PhD, Department of Surgery, University of Texas Medical Branch, Shriners Hospitals for Children, 815 Market Street, Galveston, Texas 77550, Phone: (409) 770-6990, Fax: (409) 770-6508, E-mail: elenglan@utmb.edu.

Publisher's Disclaimer: This is a PDF file of an unedited manuscript that has been accepted for publication. As a service to our customers we are providing this early version of the manuscript. The manuscript will undergo copyediting, typesetting, and review of the resulting proof before it is published in its final citable form. Please note that during the production process errors may be discovered which could affect the content, and all legal disclaimers that apply to the journal pertain.

One mode of tissue adaptation to energy demands occurs via modulation of mitochondrial activities, mitochondrial biogenesis or both. In the mature organism, mitochondrial biogenesis may occur as a compensatory mechanism in compromised oxygenation including, chronic pathological states, acclimatization to high altitude, and intense exercise [10–13], as well as long-term inhalation of cigarette smoke [14]. Interestingly, in the aging brain, increased mtDNA content may coincide with reduced mitochondrial RNA levels, suggestive of inefficient compensatory mechanism, inadvertently contributing to aging of the brain [15]. Mitochondrial modulations have been also described under conditions of acute oxidative stress, induced for example by hyperbaric oxygen [16] or following oxidant injury in ischemia and reperfusion [17]. Furthermore, in *in vitro* models of oxidative stress, mitochondrial biogenesis has been noted in response to H₂O₂ [18] and in replicative senescence [19]. Thus, mitochondrial biogenesis may represent a broad compensatory mechanism designed to aid meet energetic demands in diverse tissues and cells [20]. Interestingly, a new study suggests that caloric restriction promotes mitochondrial biogenesis in a nitric oxide (NO) dependent manner since endothelial nitric oxide synthase (eNOS^{-/-}) knockout mice fail to increase biogenesis under conditions of caloric restriction [21]. It is noteworthy, that the diverse effects of NO on mitochondria are strictly dose dependent [22] as earlier reports have demonstrated that high levels of NO may acutely inhibit respiration [21,23].

In the course of postnatal neurodevelopment in rodents, gradual changes occur in numerical and structural mitochondrial parameters as well as in respiratory enzyme activities. Mitochondria change markedly; the low neuronal mitochondrial content measured in the early neonatal rat brain (P0–P5) significantly increases during progression from the P5 to the P15 stage of development. Morphological studies show that cross section of the mitochondrion as well as the number of mitochondria per cell increase significantly through postnatal day P21 [24]. In our experimental setting, a sustained mild hypoxia lasting from P3 through P14 produced significantly depressed rates of body and brain weight gains in hypoxic P14 pups when compared to pups reared under normoxic conditions. Interestingly, this was accompanied by an elevation in expression and protein levels of nuclear respiratory factor-1 (NRF-1) and mitochondrial transcription factor A (Tfam), as well as an increase in mtDNA content in the hypoxic when compared to normoxic P14 pup brain. This suggests that mitochondrial biogenesis might be stimulated by sustained hypoxia, plausibly as compensatory mechanism designed to aid meet in part bioenergetic requirements of growth and development.

METHODS

A. Sustained hypoxia model in the neonatal rat

An adaptation of a neonatal hypoxia-model [7–9] was used: individually caged dams with litters (n=8 pups/litter, Fisher 344) were maintained in airtight Plexiglas chambers (PROOX, Redfield, NY) at reduced respiratory oxygen (9.5±1.0% O₂) generated by air replacement with nitrogen using an oxygen regulator (PROOX, Redfield, NY) [25,26] or ambient air (~21% O₂, normoxia) for either 1 or 11 days. Chambers were equipped with fans and appropriate filters to remove excess CO₂. Rats were maintained in a 12-h light-dark cycle, fed *ad libitum*, and were readily visible for the duration of the experiment. Chambers were opened daily for 10 min for routine care. At sacrifice, pups were weighed; brains were swiftly harvested, weighed and processed for either tissue sectioning or snap frozen for preparation of DNA and RNA. Body weights for P4 and P14 pups reared in normoxia were determined for multiple litters and found in agreement with previous reports [27].

B. Double immunofluorescent staining

Paraffin embedded brain sections through the hippocampal region were dewaxed in xylene and rehydrated through graded ethanol series. Sections were incubated at 98°C for 30 min with

Dako's antigen retrieval solution. All subsequent incubations were performed in humidified chambers to prevent liquid loss. Cooled sections were blocked with 1% BSA in PBS containing 5% normal goat serum for two hours at room temperature. Sections were then incubated with anti-DNA monoclonal antibody AK 30-10 (Cat. CBL186, Chemicon, Temecula, CA) at 5 μ g/ml and monoclonal anti-COX-1 (Cat. A6403, Invitrogen, Carlsbad, CA) at 2 μ g/ml or with anti-nitrotyrosine antibody (cat #06-284) at 5 mg/ml and anti-MAP2 (Cat. #05-346, Upstate, Lake Placid, NY) overnight at 4°C. Incubation was followed with 4 washes in PBS (5 min each) and subsequent incubation with Alexa Fluor labeled secondary antibodies (Alexa Fluor 488 goat anti-mouse IgM, Cat. A21042, and Alexa Fluor 594 goat anti-mouse IgG, Cat. A11032, Invitrogen) at 1:400 for 30 min. After incubation sections were washed 4 times with PBS. All manipulations after the addition of the fluorescent secondary antibodies were shielded from light. Sections were briefly dried and mounted with VectaShield mounting medium to preserve fluorescent signal. Loss of brain cells was assessed with the TUNEL assay. TUNEL positive signals were generated by the terminal deoxynucleotide transferase-mediated dUTP nick end labeling of nuclear DNA with fluorescein-dUTP according to the manufacturer (Roche Biochemicals, Kit #1684817). Incorporated fluorescein-dUTP was visualized in green and nuclei were visualized in blue by 4',6 diamino-2-phenylindole (DAPI). TUNEL positive signals were counted and recorded for three non-adjacent sections from each of the normoxia or hypoxia reared pups (n=3). Counting was blinded, recorded as TUNEL positives per 300 nuclei and analyzed by t-test. Sections were examined and captured with an Olympus IX71 microscope with epifluorescence using a 40X UPlanFLN objective or by Zeiss LSM510 META laser scanning confocal microscope with a 63X/1.4 objective.

C. Malondialdehyde (MDA) measurements

Tissue MDA content was determined using the Bioxytech MDA-586 kit (OxisResearch, Portland, OR), based on a reaction of the chromogenic *N*-methyl-2-phenylindole with MDA, according to manufacturer's instructions. Briefly, snap-frozen cerebra from control pups and pups reared under hypoxic conditions (n=3) were homogenized in four volumes of 20 mM Tris, 10 mM EDTA, pH 7.6 buffer containing 5 mM butylated hydroxytoluene. Absolute concentrations were determined from standard curves generated with known amounts of MDA and calculated per mg protein.

D. Mitochondrial DNA content

Relative mtDNA content was measured using long-range PCR-mediated quantitation method. Briefly, DNA was isolated from rat cerebrum; DNA quality was assessed on agarose gels by ethidium bromide staining. DNA was quantified by PicoGreen (Molecular Probes) fluorescence with Tecan's GENIOS microplate reader (excitation: 485, emission: 518 nm). For mtDNA, primers spanning the 16 kb rat mt genome (Genebank# NC_001665, sense 5'-CCTCCCATTCATTATCGCCGCCCTTGC-3' and antisense, 5'-GATGGGGCCGGTAGGTCGATAAAGGAG-3') and for nuclear DNA primers spanning the 12 kb rat clusterin gene locus (NC_005114) [28] were used. Primers spanning the 6 kb human β -globin locus (Genebank# U01317, sense 5'-CAGAACAGCAAATGCCTACAAGCCC-3' and antisense 5'-TATGCTGGTCTGTCCTCCCTGCTC-3') were used as an internal PCR amplification control. Linearity range for amplification was determined for nuclear and mitochondrial targets to ensure that under selected PCR conditions, amplification was linearly dependent on template availability. Accordingly, reactions were assembled with 40 ng rat and 30 ng human DNA. Amplification was by 25 cycles (15 sec at 94°C, 15 min at 68°C) in a 20 μ l reaction volume assembled with 0.75 μ Ci of 3,000 Ci/mM [α -³²P]dCTP, 500 μ M dNTPs, 400 nM primer and 2.0 U enzyme using the Expand 20 kb ^{plus} PCR System (Roche Diagnostics). Products were resolved in 0.7% agarose gels and quantified using the ImageQuant software on Phosphorimager (Molecular Dynamics). Amplification counts for normoxic and hypoxic pups sacrificed at P4 and P14 (n=4) were generated by quantification

of 3 PCR reactions per sample, normalized to amplification of the human μ -globin locus and expressed as mean \pm SD.

E. RT-PCR

RNA was prepared using TRI Reagent (Cat. #T9424, Sigma, St. Louis, MO). RT for PCR kit (Cat. #K1402-2, BD Bioscience, Palo Alto, CA) was used with 1 μ g of total RNA and random hexamers to prime reverse transcription reaction for the first strand cDNA synthesis. Aliquots of cDNA templates generated by reverse transcription of 20–50 ng total RNA were used in each PCR reaction (94°C for 15 sec, 58°C for 15 sec and 72°C for 45 sec, 26–30 cycles, depending on target gene) (Table 1). PCR products were resolved in 1% agarose gels and analyzed by BioRad ChemiDoc XRS Image station with Quantity One software.

F. Western blotting

Protein extraction was with RIPA buffer (1% NP-40, 0.5% sodium deoxycholate, 0.1% SDS in PBS, 1 mM PMSF and complete protease inhibitor cocktail from Roche). Antibodies: polyclonal goat anti Tfam sc-23588 and rabbit anti NRF-1 sc-33771 were from Santa Cruz, anti- β actin monoclonal antibody was from Sigma (AC-74, Cat. #A-5316).

RESULTS

Hypoxic rearing of pups P3 through P14 induces oxidative stress in the brain

Significantly lower body and brain weights were recorded for P14 and P7 pups following sustained hypoxia initiated on postnatal day three (9.5% \pm 1.0% O₂) while no significant differences in brain and body weights were detected after a short 24-h hypoxic exposure (P3 through P4) (Table 2). Similarly reduced brain weight gains, suggestive of inability to meet energetic demands of normal growth and neurodevelopment were reported previously in settings of sustained neonatal hypoxia in mouse [7,8] and rat models [29,30].

To learn to what extent sustained hypoxia may induce oxidative stress in the brain, we assessed markers of lipid peroxidation and protein nitration. The content of malondialdehyde (MDA), a product of lipid peroxidation and salient biomarker of oxidative stress, increased in neonatal cerebrum by ~30% after a 24-h hypoxic exposure, P3–P4 (91 \pm 9 versus 70 \pm 2 pmol/mg protein for normoxia) and by ~55% after sustained 11-day hypoxia, P3–P14 (146 \pm 18 versus 90 \pm 11 pmol/mg protein, n=3). Interestingly, the basal levels of MDA were somewhat higher in the P14 when compared to the P4 neonate brain. Substantial lipid peroxidation has been reported in brain ischemia/reperfusion and other insults with a broad range of effects ranging from modulation of gene expression to induction of DNA damage [31].

Sustained 11-day hypoxia also induced protein nitration, as reflected in increased of 3-nitrotyrosine (3-NT) immunoreactivity in certain brain regions, including cortical layer V, in the hypoxia- compared to normoxia-reared P14 pups (Figure 1A). The increased 3-NT immunoreactivity observed in cortical layer V was further analyzed by double immunofluorescence and found to coincide with cells staining for the neuronal marker MAP2 (Figure 1B). Generally, protein nitration is associated with increased production of nitric oxide and considered a biomarker for elevated oxidative stress. Since effects of NO may vary in a dose-dependent manner, using the TUNEL assay, we assessed whether in our system elevated nitrotyrosine staining coincides with increased cell death (Figure 1C). Three non-adjacent sections were analyzed for each normoxic and hypoxic brain (n=3). Although the number of TUNEL positive cells was slightly higher in hypoxia compared to normoxia, the difference between the means did not reach statistical significance at P<0.05 (2.3% \pm 0.20 vs. 2.1% \pm 0.15).

Sustained neonatal hypoxia modulates RNA and protein levels of transcription factors implicated in mitochondrial DNA replication and transcription

In the neonatal rodent, brain mitochondrial maturation continues postnatally with the mitochondrial content increasing nearly 2-fold during the neonatal period between P5 and P15 [24]. Accordingly, it was of interest to determine whether this process might be accelerated under hypoxic conditions to partly offset unmet energy demands. Since several transcription factors have been implicated in control of mitochondrial biogenesis, their brain RNA levels were compared under hypoxic and normoxic conditions. We measured expression of the peroxisome proliferator-activated receptor γ coactivator-1 α (PGC-1 α), which was initially identified as an inducible modulator of adaptive thermogenesis via enhancement of the nuclear respiratory factor-1 (NRF-1) mediated activation of the mitochondrial transcription factor A (Tfam) [32]. In our setting of sustained neonatal hypoxia, a ~200% and 50% increases in NRF-1 and Tfam mRNA levels, respectively, were observed in the hypoxic compared to normoxic P14 brain (Figure 2A). Furthermore, corresponding Western blotting analyses revealed markedly higher levels of the NRF-1 and a modest increase in the level of Tfam protein in the hypoxic compared to normoxic P14 brain (n=4) (Figure 2B). These changes, however, were not accompanied by measurable changes in PGC-1 α mRNA levels (Figure 2A). Interestingly, recently PGC-1 α acetylation status, rather than its expression level has been implicated in control of cardiac mitochondrial function [33], glucose metabolism [34] and improved mitochondrial function in obese mice [35].

Mitochondrial DNA content increases in the brain of pups reared under hypoxic conditions from P3 through P14

To assess to what extent increase in levels of NRF-1 and Tfam may associate with mitochondrial biogenesis, we compared the mitochondrial DNA content in pups reared under hypoxic and normoxic conditions. Two independent approaches were used: long-range PCR-mediated quantitation and immunohistochemical analyses. In agreement with predictions, the PCR-based assay revealed that mtDNA content in the developing brain increases ~1.7 fold for P14 when compared to the P4 brain. Importantly however, we observed also an additional ~1.25-fold increase in brain mtDNA content in P14 pups reared for 11 days in hypoxia when compared to mtDNA content of P14 pups reared under normoxic conditions (Figure 3). No such difference was observed for the hypoxic P4 brain after a 24-h hypoxic exposure. As expected, levels of nuclear DNA remained unchanged following hypoxic rearing (Figure 3). To further examine the measured increase in mtDNA content in the P14 brain after 11 days of sustained hypoxia, we assessed mtDNA immunoreactivity under these conditions. Sections examined by double immunofluorescent staining with anti-DNA and anti-COX-1 (a complex IV subunit) antibodies revealed punctate cytoplasmic fluorescence for both DNA (green) and COX-1 (red). Immunoreactivity for the mitochondria-encoded COX-1 appeared slightly stronger in the hypoxic pup, but this increase was not apparent in Western blotting analyses (not shown), suggesting that differences might be small and/or localized and thus below sensitivity of detection. Confocal analysis revealed elevated mtDNA content observed as higher density of mtDNA staining in neurons in the hypoxic when compared to normoxic P14 cortex (Figure 4). Consistently with confocal images obtained in our study, previous analyses of mtDNA distribution in cultured cells also revealed a rather limited colocalization of mtDNA and mitochondrial respiratory/oxidative enzymes, with a more significant colocalization of mtDNA with proteins involved in mtDNA transactions [36–38]. To our knowledge, this is the first immunohistochemical imaging of mtDNA distribution in neuronal cells in the brain.

DISCUSSION

Sustenance of normal growth and development relies on perinatal oxygen and nutrient availability. To improve the understanding of neurodevelopmental deficits associated with

placental insufficiency or preterm birth in humans [1–3], rodent models of sublethal neonatal hypoxia have been established [4,5,7,8]. While commonly neurodevelopmental problems dominate outcomes in these models, in some cases ameliorations of deficits have been observed and occasionally linked to enhanced neurogenesis [29,39–41]. Here, using a model of sustained neonatal hypoxia in the rat, we report an increase in mtDNA content in the hypoxic P14 brain, suggestive of increased mitochondrial biogenesis. Increased mitochondrial biogenesis may help partially compensate for reduced oxygen availability in the developing brain.

Generally, rates of mitochondrial biogenesis reflect regulation of mitochondrial numbers, activities and turnover to meet specific energetic demands [10]. Mitochondrial biogenesis may be accelerated in the perinatal period and in the adult in response to changing energetics needs [13,42]. Recently, NO was identified as a central molecule in mitochondrial biogenesis [23]. This proposed role of NO underscores the dose-dependent nature of NO actions in the various aspects of cell signaling and respiratory regulation [43,44]. The central role of endogenous NO in mitochondrial biogenesis was first proposed because mice lacking endothelial nitric oxide synthase (eNOS), failed to appropriately increase their mitochondrial content in brown adipose tissue in response to a cold challenge [45]. The role of NO in mitochondrial biogenesis was further corroborated by demonstrating that caloric restriction (CR) can induce mitochondrial biogenesis in an eNOS dependent manner [21] and that mitochondrial biogenesis is diminished in both, eNOS lacking mutant mice [21] and in obese rodents where endogenous eNOS levels are significantly reduced [46]. Interestingly, in the case of neuronal NO synthase-knockout mice, although the overall mitochondrial content remained unchanged, mitochondrial density in cortical neurons was reduced, suggesting that NOS isoforms may differentially influence NO levels and distribution in the brain, thereby affecting mitochondrial biogenesis in a tissue/cell type specific manner [47].

In agreement with previous studies, diminished weight gain rates were observed in our setting of sustained neonatal hypoxia. Unexpectedly, however, we found that mtDNA content increased in the hypoxic P14 brain, potentially reflecting stimulation of mitochondrial biogenesis. Furthermore, we observed an increase in nitrotyrosine immunoreactivity in neurons, plausibly reflecting protein nitration associated with elevated tissue levels of NO that was not accompanied by increased rates of cell death. Since recent findings indicate that NO is an important inducer of mitochondrial biogenesis [23] it is plausible that it is also involved in hypoxia associated mitochondrial biogenesis in the neonate pup. One explanation may be related to the limited body weight gain in the hypoxic pup, which might reflect a certain extent of caloric restriction. Although adequate nutrients availability is ensured in this model, hypoxia-associated changes in pups feeding behavior have not been investigated so far [7], and therefore, cannot be excluded as a contributory factor. Thus here, caloric restriction/ altered feeding behavior might contribute to an elevation of NO as previously reported in a different model [21]. Interestingly, it has been also proposed that NO from different sources may preferentially target specific cell types [47]. It is therefore, plausible that localized increase in neuronal mtDNA content by hypoxia is greater than that measured by PCR. In fact, this is consistent with our immunohistochemical analyses that show a significantly higher density of mtDNA staining in cortical neurons. Taken together, our data suggest that mitochondrial biogenesis may represent an adaptive protective mechanism designed to diminish the impact of compromised oxygenation on neurodevelopment. It is noteworthy, that the neonatal brain may be uniquely equipped to support mitochondrial biogenesis because mitochondrial maturation and biogenesis are integral to normal neurodevelopment [24]. It would be of interest to assess whether hypoxia associated increase in mtDNA content is abolished in the absence of normal NOS activities. If this turns out to be the case, control of mitochondrial biogenesis rates may become a target for future therapeutic strategies to reduce impact of placental insufficiency and preterm birth.

Acknowledgments

Support: March of Dimes Birth Defects Foundation, NIH NINDS 39449 and Shriners 8670 grants

Abbreviations

mtDNA	mitochondrial DNA
COX-1	cytochrome c oxidase subunit-1
Tfam	mitochondrial transcription factor A
NO	nitric oxide
PGC-1α	proliferator-activated receptor γ coactivator-1 α
NRF-1	nuclear respiratory factor-1
eNOS	endothelial nitric oxide synthase
P	postnatal day

References

1. Miller SP, Ramaswamy V, Michelson D, Barkovich AJ, Holshouser B, Wycliffe N, Glidden DV, Deming D, Partridge JC, Wu YW, Ashwal S, Ferriero DM. Patterns of brain injury in term neonatal encephalopathy. *J Pediatr* 2005;146:453–460. [PubMed: 15812446]
2. Jensen FE. Developmental factors regulating susceptibility to perinatal brain injury and seizures. *Curr Opin Pediatr* 2006;18:628–633. [PubMed: 17099361]
3. Perlman JM. Intervention strategies for neonatal hypoxic-ischemic cerebral injury. *Clin Ther* 2006;28:1353–1365. [PubMed: 17062309]
4. Vannucci RC, Rossini A, Towfighi J, Vannucci SJ. Measuring the accentuation of the brain damage that arises from perinatal cerebral hypoxia-ischemia. *Biol Neonate* 1997;72:187–191. [PubMed: 9303218]
5. Vannucci RC, Vannucci SJ. A model of perinatal hypoxic-ischemic brain damage. *Ann N Y Acad Sci* 1997;835:234–249. [PubMed: 9616778]
6. Yager JY, Brucklacher RM, Vannucci RC. Paradoxical mitochondrial oxidation in perinatal hypoxic-ischemic brain damage. *Brain Res* 1996;712:230–238. [PubMed: 8814897]
7. Ment LR, Schwartz M, Makuch RW, Stewart WB. Association of chronic sublethal hypoxia with ventriculomegaly in the developing rat brain. *Brain Res Dev Brain Res* 1998;111:197–203.
8. Curristin SM, Cao A, Stewart WB, Zhang H, Madri JA, Morrow JS, Ment LR. Disrupted synaptic development in the hypoxic newborn brain. *Proc Natl Acad Sci U S A* 2002;99:15729–15734. [PubMed: 12438650]
9. Back SA, Craig A, Ling Luo N, Ren J, Akundi RS, Ribeiro I, Rivkees SA. Protective effects of caffeine on chronic hypoxia-induced perinatal white matter injury. *Ann Neurol* 2006;60:696–705. [PubMed: 17044013]

10. McLeod CJ, Pagel I, Sack MN. The mitochondrial biogenesis regulatory program in cardiac adaptation to ischemia--a putative target for therapeutic intervention. *Trends Cardiovasc Med* 2005;15:118–123. [PubMed: 16039972]
11. Vogt M, Puntchart A, Geiser J, Zuleger C, Billeter R, Hoppeler H. Molecular adaptations in human skeletal muscle to endurance training under simulated hypoxic conditions. *J Appl Physiol* 2001;91:173–182. [PubMed: 11408428]
12. Wright DC, Han DH, Garcia-Roves PM, Geiger PC, Jones TE, Holloszy JO. Exercise-induced mitochondrial biogenesis begins before the increase in muscle PGC-1alpha expression. *J Biol Chem* 2007;282:194–199. [PubMed: 17099248]
13. Civitaresse AE, Carling S, Heilbronn LK, Hulver MH, Ukropcova B, Deutsch WA, Smith SR, Ravussin E. Calorie Restriction Increases Muscle Mitochondrial Biogenesis in Healthy Humans. *PLoS Med* 2007;4:e76. [PubMed: 17341128]
14. Masayeva BG, Mambo E, Taylor RJ, Goloubeva OG, Zhou S, Cohen Y, Minhas K, Koch W, Sciubba J, Alberg AJ, Sidransky D, Califano J. Mitochondrial DNA content increase in response to cigarette smoking. *Cancer Epidemiol Biomarkers Prev* 2006;15:19–24. [PubMed: 16434581]
15. Barrientos A, Casademont J, Cardellach F, Estivill X, Urbano-Marquez A, Nunes V. Reduced steady-state levels of mitochondrial RNA and increased mitochondrial DNA amount in human brain with aging. *Brain Res Mol Brain Res* 1997;52:284–289. [PubMed: 9495550]
16. Gutsaeva DR, Suliman HB, Carraway MS, Demchenko IT, Piantadosi CA. Oxygen-induced mitochondrial biogenesis in the rat hippocampus. *Neuroscience* 2006;137:493–504. [PubMed: 16298077]
17. Rasbach KA, Schnellmann RG. Signaling of mitochondrial biogenesis following oxidant injury. *J Biol Chem* 2006;282:2355–2362. [PubMed: 17116659]
18. Lee HC, Yin PH, Lu CY, Chi CW, Wei YH. Increase of mitochondria and mitochondrial DNA in response to oxidative stress in human cells. *Biochem J* 2000;348 Pt 2:425–432. [PubMed: 10816438]
19. Lee HC, Yin PH, Chi CW, Wei YH. Increase in mitochondrial mass in human fibroblasts under oxidative stress and during replicative cell senescence. *J Biomed Sci* 2002;9:517–526. [PubMed: 12372989]
20. Lee HC, Wei YH. Mitochondrial biogenesis and mitochondrial DNA maintenance of mammalian cells under oxidative stress. *Int J Biochem Cell Biol* 2005;37:822–834. [PubMed: 15694841]
21. Nisoli E, Tonello C, Cardile A, Cozzi V, Bracale R, Tedesco L, Falcone S, Valerio A, Cantoni O, Clementi E, Moncada S, Carruba MO. Calorie restriction promotes mitochondrial biogenesis by inducing the expression of eNOS. *Science* 2005;310:314–317. [PubMed: 16224023]
22. Laczka Z, Pankotai E, Csordas A, Gero D, Kiss L, Horvath EM, Kollai M, Busija DW, Szabo C. Mitochondrial NO and reactive nitrogen species production: does mtNOS exist? *Nitric Oxide* 2006;14:162–168. [PubMed: 16051505]
23. Nisoli E, Carruba MO. Nitric oxide and mitochondrial biogenesis. *J Cell Sci* 2006;119:2855–2862. [PubMed: 16825426]
24. Sato I, Konishi K, Mikami A, Sato T. Developmental changes in enzyme activities and in morphology of rat cortex mitochondria. *Okajimas Folia Anat Jpn* 2000;76:353–361. [PubMed: 10774233]
25. Englander EW, Greeley GH, Wang G, Perez-Polo JR, Lee HM. Hypoxia-induced mitochondrial and nuclear DNA damage in the rat brain. *J Neurosci Res* 1999;58:262–269. [PubMed: 10502282]
26. Englander EW, Hu Z, Sharma A, Lee HM, Wu ZH, Greeley GH. Rat MYH, a glycosylase for repair of oxidatively damaged DNA, has brain-specific isoforms that localize to neuronal mitochondria. *J Neurochem* 2002;83:1471–1480. [PubMed: 12472901]
27. Garey J, Ferguson SA, Paule MG. Developmental and behavioral effects of acrylamide in Fischer 344 rats. *Neurotoxicol Teratol* 2005;27:553–563. [PubMed: 16087067]
28. Wang G, Hazra TK, Mitra S, Lee HM, Englander EW. Mitochondrial DNA damage and a hypoxic response are induced by CoCl₂ in rat neuronal PC12 cells. *Nucleic Acids Res* 2000;28:2135–2140. [PubMed: 10773083]
29. Fagel DM, Ganat Y, Silbereis J, Ebbitt T, Stewart W, Zhang H, Ment LR, Vaccarino FM. Cortical neurogenesis enhanced by chronic perinatal hypoxia. *Exp Neurol* 2006;199:77–91. [PubMed: 15916762]

30. Schwartz ML, Vaccarino F, Chacon M, Yan WL, Ment LR, Stewart WB. Chronic neonatal hypoxia leads to long term decreases in the volume and cell number of the rat cerebral cortex. *Semin Perinatol* 2004;28:379–388. [PubMed: 15693394]
31. Chen L, Lee HM, Greeley GH Jr, Englander EW. Accumulation of oxidatively generated DNA damage in the brain: a mechanism of neurotoxicity. *Free Radic Biol Med* 2007;42:385–393. [PubMed: 17210451]
32. Puigserver P, Wu Z, Park CW, Graves R, Wright M, Spiegelman BM. A cold-inducible coactivator of nuclear receptors linked to adaptive thermogenesis. *Cell* 1998;92:829–839. [PubMed: 9529258]
33. Czubryt MP, McAnally J, Fishman GI, Olson EN. Regulation of peroxisome proliferator-activated receptor gamma coactivator 1 alpha (PGC-1 alpha) and mitochondrial function by MEF2 and HDAC5. *Proc Natl Acad Sci U S A* 2003;100:1711–1716. [PubMed: 12578979]
34. Lerin C, Rodgers JT, Kalume DE, Kim SH, Pandey A, Puigserver P. GCN5 acetyltransferase complex controls glucose metabolism through transcriptional repression of PGC-1alpha. *Cell Metab* 2006;3:429–438. [PubMed: 16753578]
35. Lagouge M, Argmann C, Gerhart-Hines Z, Meziane H, Lerin C, Daussin F, Messadeq N, Milne J, Lambert P, Elliott P, Geny B, Laakso M, Puigserver P, Auwerx J. Resveratrol improves mitochondrial function and protects against metabolic disease by activating SIRT1 and PGC-1alpha. *Cell* 2006;127:1109–1122. [PubMed: 17112576]
36. Scheer U, Messner K, Hazan R, Raska I, Hansmann P, Falk H, Spiess E, Franke WW. High sensitivity immunolocalization of double and single-stranded DNA by a monoclonal antibody. *Eur J Cell Biol* 1987;43:358–371. [PubMed: 3305019]
37. Legros F, Malka F, Frachon P, Lombes A, Rojo M. Organization and dynamics of human mitochondrial DNA. *J Cell Sci* 2004;117:2653–2662. [PubMed: 15138283]
38. Wang Y, Bogenhagen DF. Human mitochondrial DNA nucleoids are linked to protein folding machinery and metabolic enzymes at the mitochondrial inner membrane. *J Biol Chem* 2006;281:25791–25802. [PubMed: 16825194]
39. Stewart WB, Ment LR, Schwartz M. Chronic postnatal hypoxia increases the numbers of cortical neurons. *Brain Res* 1997;760:17–21. [PubMed: 9237513]
40. Yang Z, Levison SW. Hypoxia/ischemia expands the regenerative capacity of progenitors in the perinatal subventricular zone. *Neuroscience* 2006;139:555–564. [PubMed: 16500031]
41. Felling RJ, Snyder MJ, Romanko MJ, Rothstein RP, Ziegler AN, Yang Z, Givogri MI, Bongarzone ER, Levison SW. Neural stem/progenitor cells participate in the regenerative response to perinatal hypoxia/ischemia. *J Neurosci* 2006;26:4359–4369. [PubMed: 16624956]
42. Zaobornyj T, Gonzales GF, Valdez LB. Mitochondrial contribution to the molecular mechanism of heart acclimatization to chronic hypoxia: role of nitric oxide. *Front Biosci* 2007;12:1247–1259. [PubMed: 17127451]
43. Palacios-Callender M, Hollis V, Frakich N, Mateo J, Moncada S. Cytochrome c oxidase maintains mitochondrial respiration during partial inhibition by nitric oxide. *J Cell Sci* 2007;120:160–165. [PubMed: 17164295]
44. Moncada S, Bolanos JP. Nitric oxide, cell bioenergetics and neurodegeneration. *J Neurochem* 2006;97:1676–1689. [PubMed: 16805776]
45. Nisoli E, Clementi E, Paolucci C, Cozzi V, Tonello C, Sciorati C, Bracale R, Valerio A, Francolini M, Moncada S, Carruba MO. Mitochondrial biogenesis in mammals: the role of endogenous nitric oxide. *Science* 2003;299:896–899. [PubMed: 12574632]
46. Valerio A, Cardile A, Cozzi V, Bracale R, Tedesco L, Pisconti A, Palomba L, Cantoni O, Clementi E, Moncada S, Carruba MO, Nisoli E. TNF-alpha downregulates eNOS expression and mitochondrial biogenesis in fat and muscle of obese rodents. *J Clin Invest* 2006;116:2791–2798. [PubMed: 16981010]
47. Schild L, Jaroscakova I, Lendeckel U, Wolf G, Keilhoff G. Neuronal nitric oxide synthase controls enzyme activity pattern of mitochondria and lipid metabolism. *Faseb J* 2006;20:145–147. [PubMed: 16246868]

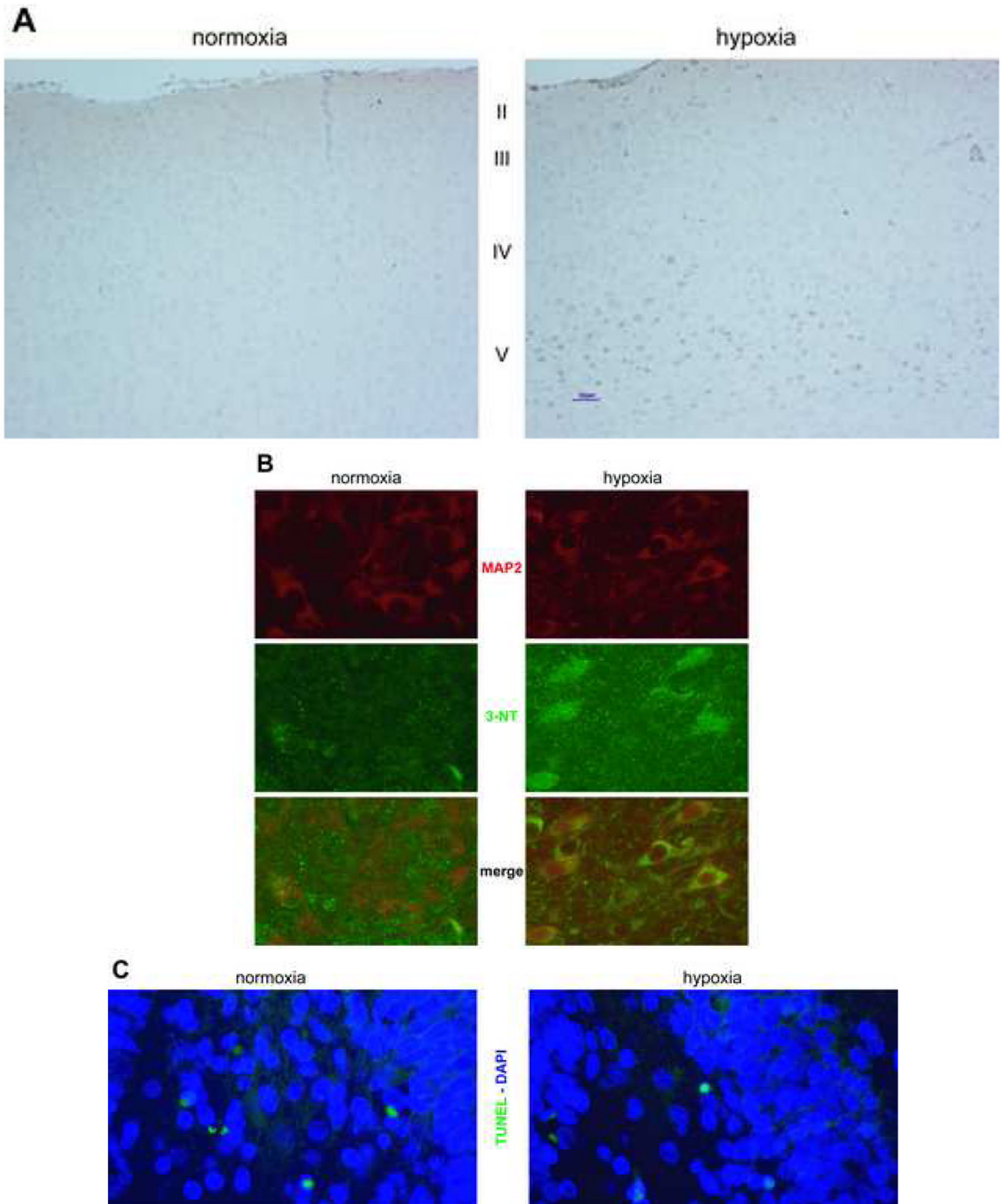


Figure 1. 3-nitrotyrosine (3-NT) immunoreactivity is induced by sustained hypoxia in the neonatal P14 brain

A) Anti 3-NT monoclonal antibody reacted with sections from P14 brains shows increased immunoreactivity in the hypoxic compared to normoxic P14 brain. Increased immunoreactivity is evident in large cortical neurons in layers IV–V (nuclei are counterstained blue with hematoxylin). **B)** Photomicrographs of fluorescent double staining for the neuronal marker MAP2 (red) and 3-NT (green) in cortical neurons. In merged images from hypoxic brains neuronal MAP2 staining coincides with 3-NT fluorescence. **C)** TUNEL positive staining is seen in green while nuclear DNA morphology is visualized with DAPI in blue.

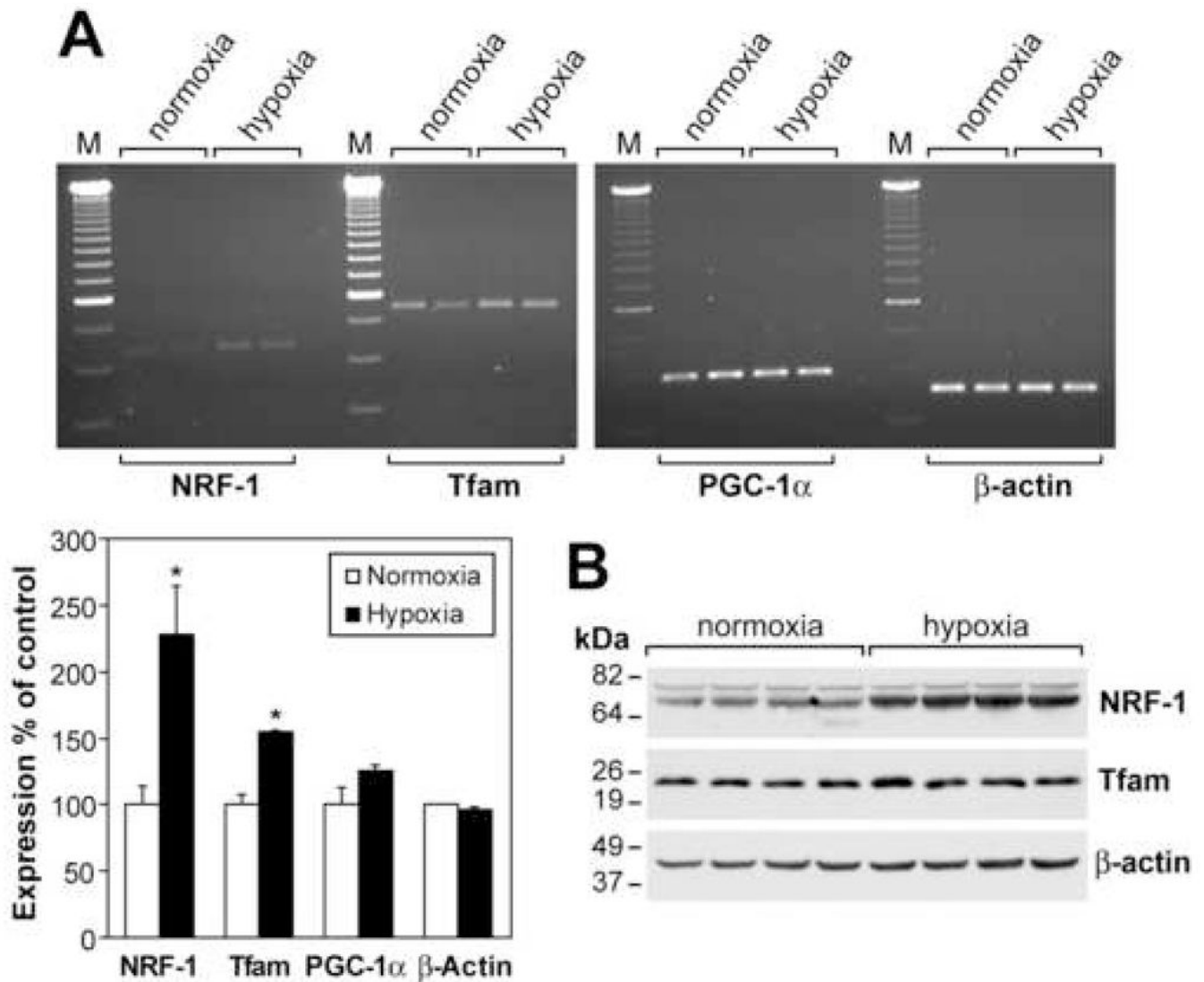


Figure 2. mRNA and protein levels of transcription factors associated with mitochondrial biogenesis are elevated in neonatal hypoxic brain

A) RT-PCR reaction products generated with RNA isolated from normoxic and hypoxic P14 brains (n=4) are shown for the nuclear PGC-1 α and NRF-1 and the mitochondrial transcription factor A Tfam. Bar graphs represent relative signal intensities captured and analyzed by BioRad ChemiDoc XRS Image station with Quantity One software obtained for 3 PCR amplification for each reverse transcription reaction and expressed as mean \pm SD. * denotes different from normoxic P14, $P < 0.05$. **B)** Corresponding Western blotting analyses of NRF-1 and Tfam in protein extracts prepared from normoxic and hypoxic P14 brains (n=4). Molecular weight range is indicated for reference and β -actin signal is shown as loading control.

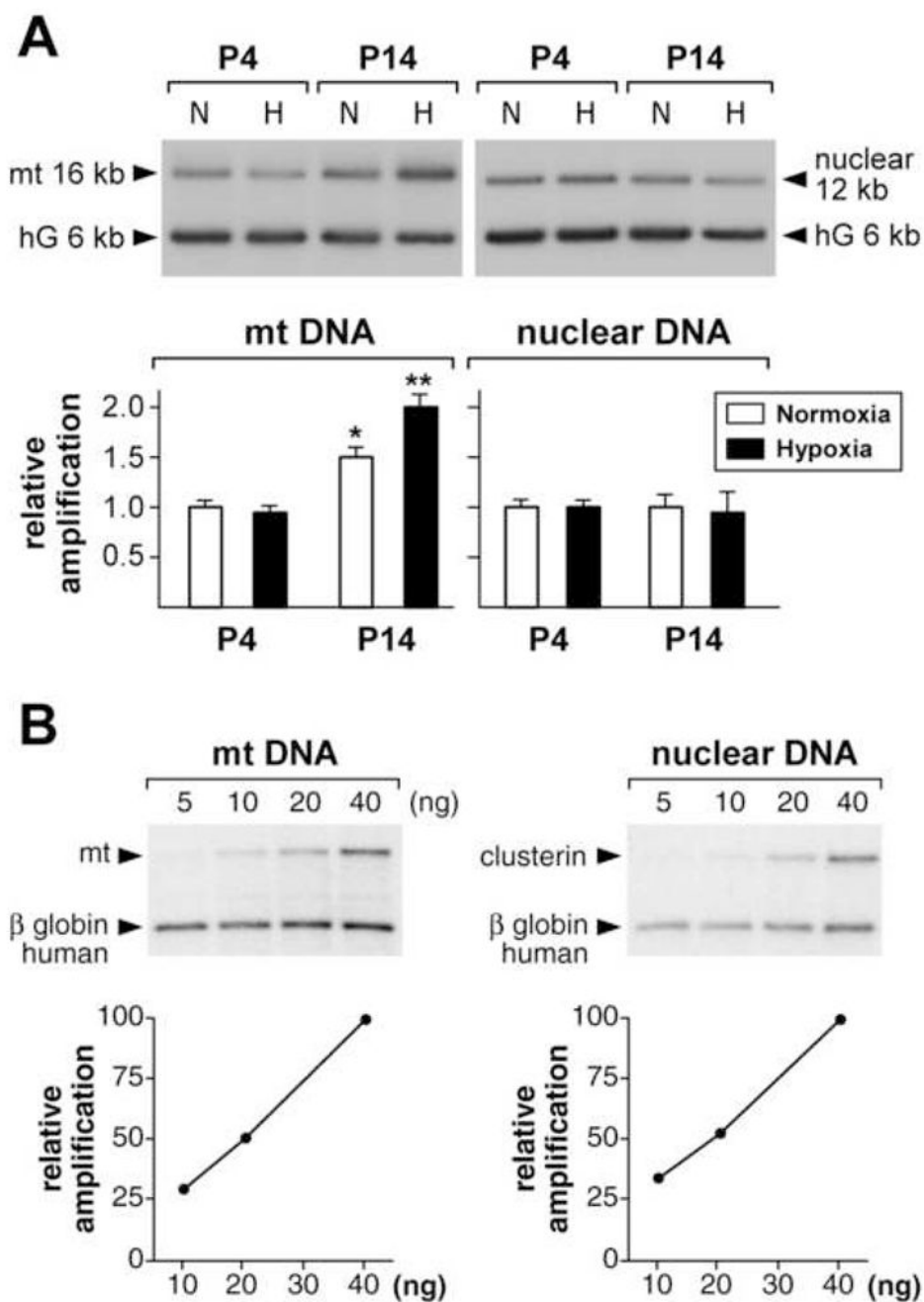


Figure 3. Sustained neonatal hypoxia modulates mitochondrial DNA content in the developing brain

A) Representative autoradiograms show PCR yields generated by amplification of mitochondrial and nuclear DNA isolated from normoxic and hypoxic P4 and P14 brains. mtDNA amplification yields are higher with P14 DNA when compared to P4. In addition, mtDNA amplification yields are higher for the hypoxic compared to normoxic P14 brain, while yields from amplification of the nuclear locus remain unchanged. Lower panel shows relative amplification yields normalized to an internal control (amplification product of the human globin locus) for each PCR reaction and expressed as mean \pm SD ($n = 3$, triplicate PCR). * denotes different from P4 and ** different from normoxic P14, $P < 0.05$. **B)** Amplification

linearity range for the 12 kb nuclear clusterin locus and the 16 kb mt genome, under the selected PCR conditions are shown separately.

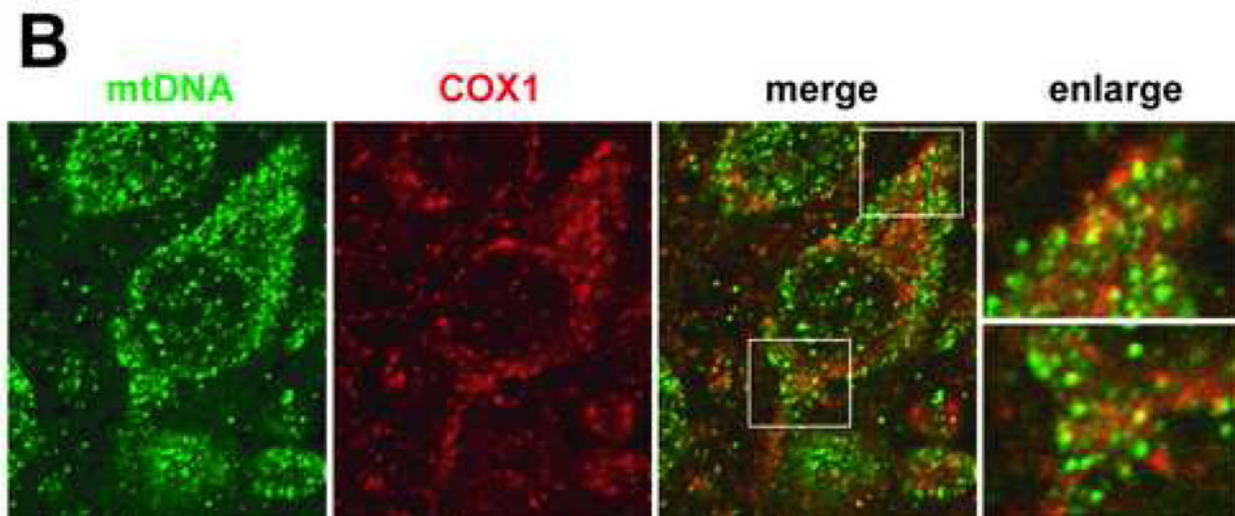
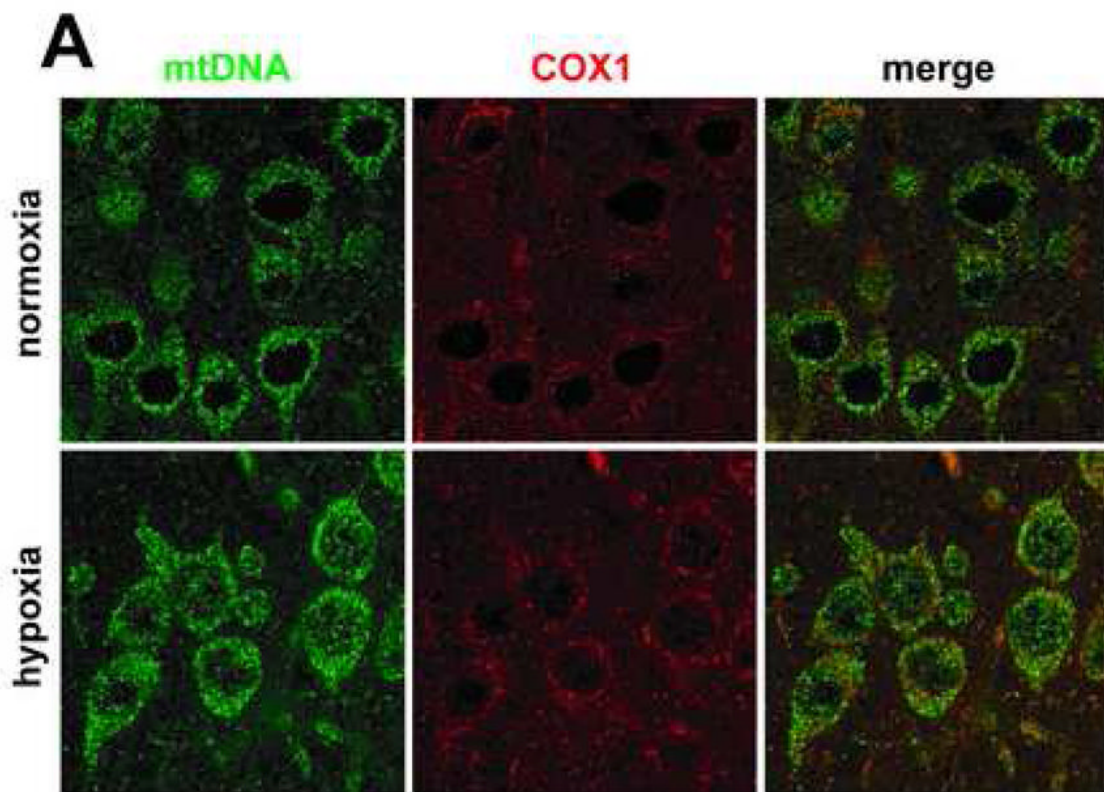


Figure 4. Sustained neonatal hypoxia leads to increases in mtDNA immunoreactivity in cortical neurons in the P14 pup brain

Confocal images of brain sections from hypoxic P14 pups reacted with anti-DNA antibody reveal a higher density of punctuated immunofluorescence (green) when compared to normoxic P14 brains. Immunoreactivity for the mitochondria encoded complex IV subunit, COX-1 is slightly intensified following hypoxia (red). Lower panel: Enlarged immunofluorescent image of a hypoxic P14 neuron double stained with anti-DNA and anti-COX-1 antibodies. Magnified merged images of demarcated areas reveal only limited colocalization (yellow) of mitochondrial DNA and COX-1.

Table 1

RT-PCR primers

Target Gene	Accession No.	Primer Sequence	Product Length
NRF1	XM_231566	5'ATGGAGGAACACGGAGTGAC3' 5'CCACAGAGACTGGAATCCCA3'	592 bp
Tfam	NM_031326	5'GGAATGTGGGGCGTGCTAAGAA3' 5'GCATTCACTGGGCAGAAGTCCA3'	869 bp
PGC-1 α	NM_031347	5'TGTGAATGACCTGGACACAGACAGCT3' 5'CGTCTTTGTGGCTTTTGCTGTTGAC3'	489 bp
β -Actin	MN_031144	5'TGCTCCTCTGAGCGCAAGTACTCT3' 5'AGAAGTTGGGGGATGTTTGCTCCA3'	385 bp

Table 2

Brain and body weights for hypoxia and normoxia reared pups

	Body weight (g)			Brain weight (g)		
	Normoxia	Hypoxia	Difference (%)	Normoxia	Hypoxia	Difference (%)
P4	7.1±0.5	6.4±0.4	10±6.5%	0.335±0.025	0.315±0.015	6.0±4.5%
P7	10.5±0.5	8.1±0.4	23±3.0%*	0.58±0.01	0.5±0.02	13.5±2.0%*
P14	20.0±1.5	10.0±0.8	50±7.7%*	1.05±0.05	0.79±0.05	24.7±3.5%*

Pups were reared under normoxic or hypoxic conditions (9.5 ± 1% O₂) starting on day 3 for 1, 4 or 11 days (n=12–20).* $P < 0.01$